

# Modeling complex systems: A case study of compartmental models in epidemiology

Pratyush K. Kolleypara<sup>1,2</sup>, Alexander F. Siegenfeld<sup>1,3</sup>, and Yaneer Bar-Yam<sup>1</sup>

<sup>1</sup>New England Complex Systems Institute, Cambridge, MA, USA

<sup>2</sup>Department of Physics, BITS Pilani K K Birla Goa Campus, Goa, India and

<sup>3</sup>Department of Physics, Massachusetts Institute of Technology, Cambridge, MA, USA

Compartmental epidemic models have been widely used for predicting the course of epidemics, from estimating the basic reproduction number to guiding intervention policies. Studies commonly acknowledge these models' assumptions but less often justify their validity in the specific context in which they are being used. Our purpose is not to argue for specific alternatives or modifications to compartmental models, but rather to show how assumptions can constrain model outcomes to a narrow portion of the wide landscape of potential epidemic behaviors. This concrete examination of well-known models also serves to illustrate general principles of modeling that can be applied in other contexts.

## I. INTRODUCTION

Compartmental models such as the SIR model have been widely used to study infectious disease outbreaks [1–5]. These models have informed policy makers of the risks of inaction and have been used to analyze various policy responses. The limitations of the assumptions of compartmental models are well-known [6–8]; we intend to explore which assumptions are appropriate in which contexts and when and why the models do or do not succeed.

No model accurately captures all the details of the system that it represents, but some models are nonetheless accurate because certain large-scale behaviors of systems do not depend on all these details [9]. (For example, modeling material phase transitions generally does not require including the quantum mechanical details of individual atoms.) The key to good modeling is understanding which details matter and which do not. Paradoxically, failing to recognize that a model can be accurate in spite of certain unrealistic assumptions can lead to models in which all assumptions are excused: the impossibility of getting all the details right may discourage a careful analysis of which assumptions are appropriate in which contexts.

During a pandemic, it is crucial that models complement decision-making. In an attempt to obtain better predictions, it may be tempting to include more details and fine-tune the model assumptions. However, focusing on irrelevant assumptions and details while losing sight of the large scale behavior is counterproductive [10]. Which details are relevant depends on the question at hand; the inclusion or exclusion of details in a model must be justified depending on the modeling objectives. Compartmental models tend to include some details (e.g. disease stages) while not including others (e.g. stochasticity and heterogeneity) that, in many cases, have a far larger effect on forecasting the epidemic trajectory, estimating the final epidemic size, and analyzing the impact of interventions.

In this work, we examine some common assumptions of compartmental models—such as the distribution of generation intervals, homogeneity in population characteristics and connectivity, and the use of continuous variables—in order to determine their relevance for various model outcomes. Our purpose is not to argue for specific alternatives to compartmental models or for specific modifications but rather to illustrate how the assumptions of these models affect their results.

## II. THE SIR MODEL

Here we introduce the SIR model. The model divides the population into three compartments—the fractions of individuals who are susceptible ( $s$ ), infected ( $i$ ), or recovered ( $r$ ). A set of three differential equations governs the dynamics:

$$\frac{ds}{dt} = -\beta si \quad (1)$$

$$\frac{di}{dt} = \beta si - \gamma i \quad (2)$$

$$\frac{dr}{dt} = \gamma i \quad (3)$$

The parameter  $\beta > 0$  is the rate at which an infected individual transmits the disease to a susceptible individual. The infected individuals become no longer infectious (recovered or removed) at a rate  $\gamma > 0$ . Assumptions of the SIR model include homogeneity in the infectiousness, susceptibility, and connectivity of the population, exponentially distributed recovery times and generation intervals, that discrete and stochastic dynamics can be approximated with continuous and deterministic variables, and that there are no changes over time in the behaviors of either the population or the infectious agent.

By recasting the equations of the model in terms of the basic reproduction number  $R_0 = \beta/\gamma$ ,

$$\frac{ds}{d(\gamma t)} = -R_0 si \quad (4)$$

$$\frac{di}{d(\gamma t)} = (R_0 s - 1)i \quad (5)$$

$$\frac{dr}{d(\gamma t)} = i \quad (6)$$

it can be seen that the evolution of the system state (i.e. the fraction of people in each of the three compartments) depends only on  $R_0$  and that  $\gamma$  sets the time scale for this evolution (i.e. a change in  $\gamma$  would correspond simply to a stretching or compression of the time axis). Indeed, it can be proven that the final size of an epidemic depends only on the network of probabilities of individuals infecting each other and not at all on how quickly individuals recover or any other time-scales associated with the progression of the disease within individuals [12–16] (see Ap-

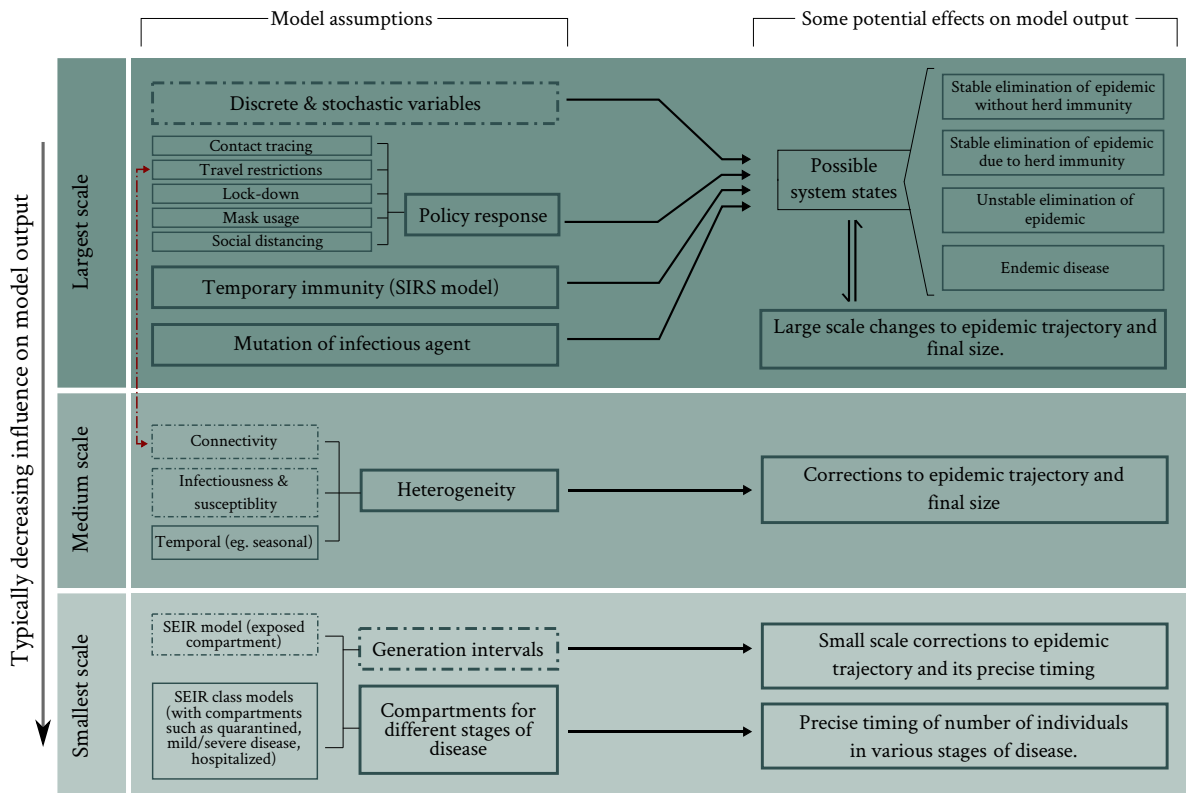


FIG. 1. Schematic representation of the impact of various modeling choices/assumptions. The left column lists various details that can be incorporated into a compartmental model (boxes with dashed borders indicate modeling choices that are analyzed in section III), and the right column lists typical potential impacts on the model output. The three panels classify the system details by ‘scale’, with the largest scale details typically having the most impact on model output, and the smallest scale details typically having the least impact, although the impact of any given assumption ultimately depends on precisely for what purpose the model is being used. For instance, an SIRS model may not be needed if only the initial growth of the epidemic is being modeled. Furthermore, various assumptions can compound non-linearly to affect the model output. For instance, policy interventions such as travel restrictions, which both rely on and affect heterogeneity in geographical connectivity, can play a decisive role in determining whether or not a stable elimination is achieved [11]. Of course, the actual effect of any assumption depends on its precise mathematical implementation, as well as the presence or absence of other assumptions within the model, and so this figure should be considered as a rough schematic rather than as a definitive guide.

pendix section 1 for more details).

This overall time-scale of the epidemic (set by  $\gamma$  in the above formulation) is an important parameter; for instance, together with  $R_0$ , it tells us how quickly case counts will grow. The SIR model describes this overall time-scale without the need for any additional compartments. Studies with additional compartments that have focused on the details of infectious periods, latent periods, and other disease stages can provide more information as to the precise timing (as opposed to simply the overall fraction) of the number of individuals in particular disease stages (e.g. exposed, infectious, hospitalized, etc.) if sufficient data is available to fit the additional parameters. This approach is useful for understanding, for instance, lags between infections and hospitalizations. However, such details will often have much smaller effects than regularly used assumptions that impact the overall epidemic trajectory, such as homogeneity, mean-field connectivity, and continuous variables (section III).

### III. ANALYSIS OF KEY ASSUMPTIONS

We now examine some key assumptions of compartmental models. In section III A, we show that assumptions concerning the distribution of generation intervals (i.e. assumptions about diseases stages, recovery rates, etc.) do not significantly affect the overall epidemic trajectory. In section III B we show how the effects of heterogeneity in susceptibility and connectivity cannot be captured by an average or effective spreading rate  $\beta$ , in contrast to how the distribution of generation intervals can be described by the effective parameter  $\gamma$ . In section III C, we discuss the implications of using continuous and deterministic variables to describe dynamics that are in reality stochastic and discrete.

#### A. SEIR models, generation intervals and effective parameters

There are some cases in which simplifying assumptions are not critical. For instance, by assuming a constant recovery rate  $\gamma$ , the SIR model makes the assumption that generation intervals

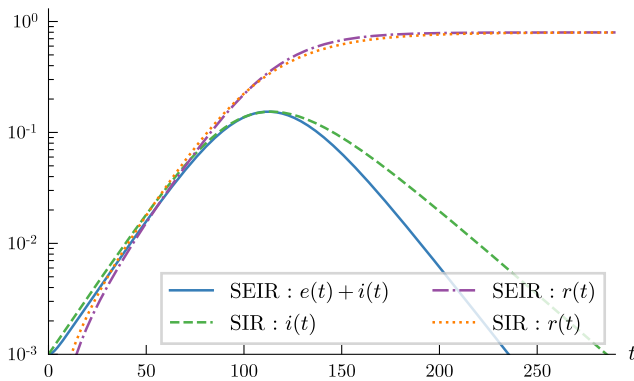


FIG. 2. An SEIR model can be replaced with an SIR model with a nearly identical trajectory. Important characteristics such as the growth rate, reproduction number, herd immunity threshold and epidemic size will be exactly the same in both models. The following parameters were used to generate this figure. SEIR:  $\beta = 0.25$ ,  $\sigma = 0.167$ ,  $\alpha = 0.125$ . SIR:  $\bar{\beta} = 0.119$ ,  $\gamma = 0.059$

follow an exponential distribution. However, the growth rate and reproduction number can nonetheless be accurately captured despite the actual generation intervals not being exponentially distributed, so long as  $\gamma$  is treated as an effective parameter. Given an observed reproduction number  $R_0$  and initial exponential growth rate  $\lambda_0$ , one may always find a  $\beta$  and  $\gamma$  such that  $R_0 = \beta/\gamma$  and  $\lambda_0 = \beta - \gamma$ . We note in this case that  $1/\gamma$  need not be the mean of the distribution of generation intervals  $g(t)$ . Instead, the relationship between  $\gamma$ ,  $\lambda_0$ , and  $R_0$  is given by

$$\frac{1}{R_0} = \int_0^{\infty} g(t)e^{-\lambda_0 t} dt \quad (7)$$

which implies that the  $\gamma$  necessary to match  $R_0$  and  $\lambda_0$  will be the inverse mean of  $g(t)$  if and only if  $g(t) = \gamma e^{-\gamma t}$  [17] (see Appendix section 2 for details).

Models with additional compartments such as SEIR models are often considered to be more accurate than the SIR model since they include a more realistic generation interval distribution (see Appendix section 3). However, the precise generation interval distribution does not affect epidemic characteristics such as the final size, the initial exponential growth rate, and  $R_0$ . As described above, these characteristics can be captured by the SIR model by treating the recovery rate  $\gamma$  as an effective parameter (see Figure 2). More generally, for the purposes of modelling the overall epidemic trajectory, introducing any number of disease stages into the SIR model only amounts to changing the effective distribution of generation intervals, which changes only the precise timing of the epidemic curve (see Appendix section 1). The SIR model is elegant in that its parameter set (the dimensionless  $R_0$  plus a time scale  $\gamma$ ) is minimal; given the larger sources of uncertainty related to other assumptions, additional parameters in SEIR models are not justified if they serve only to refine the generation interval distribution. (The use of SEIR models over the SIR model may be justified in other circumstances.)

SIR, SEIR and other compartmental models are frequently used for estimating the basic reproduction number [5], but very

often, the transition rates are not treated as effective parameters and are estimated using the inverse of mean generation, serial, latent or infectious intervals [18–24], which, as described above, is appropriate only for exponentially distributed intervals. This practice is also prevalent in other epidemic modeling literature [25–36].

## B. Population heterogeneity

Human populations are heterogeneous in many ways: social networks of individuals exhibit community structure [37–39], infectiousness and susceptibility can vary across the population depending upon age/health conditions/behavior, different regions may have different mitigation responses to an epidemic, etc. Therefore, in this section we will discuss the widely used assumption of homogeneous and well-mixed populations [25–28, 36]. The homogeneity assumption has been challenged using various types of heterogeneous models [12, 40–44], and these studies point towards a crucial result: heterogeneous models can yield very different outcomes from homogeneous models.

To summarize this impact of heterogeneous infectiousness, susceptibility, and connectivity, we use a simple class of models in which the population is partitioned into multiple groups [12, 40–44]. We briefly describe these models below (methods can be found in Appendix section 4). The purpose of these modifications is not to create a more accurate model but to show that heterogeneity and connectivity are crucial assumptions that can have a substantial effect on both the epidemic trajectory and its final size. We do not claim that any particular set of assumptions regarding heterogeneity or connectivity will accurately predict an epidemic trajectory but rather include such assumptions to show that the space of possible outcomes is far larger than homogeneous models would imply.

### 1. Heterogeneity in infectiousness and susceptibility

The SIR model assumes that individuals spread infections in a homogeneous manner. We consider three ways in which spreading can be heterogeneous. Figure 3 summarizes the results of these modifications to the model and shows that the final size can be very different despite identical initial exponential growth rates and basic reproduction numbers.

First, groups can be equally susceptible (without loss of generality,  $\eta = 1$ ) but differ in infectiousness  $\beta$ . In this case, the SIR model can effectively coarse-grain this heterogeneity by selecting the effective spreading rate  $\beta_{\text{SIR}} = \langle \beta \rangle$ , where the angled brackets indicate an average over the whole population.

Second, the groups can have the same infectiousness  $\bar{\beta}$  but differing susceptibilities  $\eta$ . By selecting the effective spreading rate  $\beta_{\text{SIR}} = \bar{\beta} \langle \eta \rangle$ , the initial growth rate and basic reproduction number can be reproduced with an SIR model. However, the SIR model will offer a substantially different prediction for later parts of the epidemic trajectory and the final epidemic size.

In the third case, both infectiousness and susceptibility vary across groups. We consider a special case of this scenario by assuming that infectiousness and susceptibility are proportional,

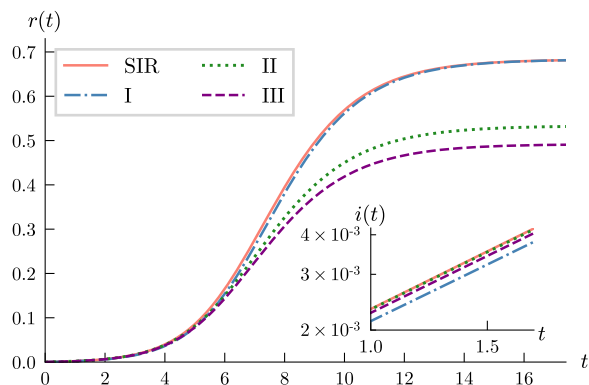


FIG. 3. Effect of different types of heterogeneity on the trajectory of an epidemic. (I) Heterogeneity in infectiousness. (II) Heterogeneity in susceptibility. (III) Heterogeneity in both infectiousness and susceptibility. All four cases have the same value of  $\gamma$  and the same initial growth rate (as shown in the inset). Despite similar initial behavior, (II) and (III) exhibit different epidemic sizes (the saturated value of  $r(t)$ ). The equations in Appendix section 4 were used to generate the trajectories.

i.e. those who are more likely to spread the disease are also more likely to contract it. For instance, a person who wears a mask more often or who socializes less will be both less likely to spread and less likely to contract the disease. Assuming both susceptibility and infectiousness are proportional to a contact parameter  $b$ , the homogeneous SIR model can reproduce the initial growth rate and basic reproduction number by selecting the effective spreading rate  $\beta_{\text{SIR}} = \langle b^2 \rangle$ . (Note that here, the effective spreading rate  $\langle b^2 \rangle$  differs from the average spreading rate  $\langle b \rangle^2$ , due to the more infectious individuals being more likely to be infected.) However, as in the previous case, the homogeneous SIR model can grossly misestimate later parts of the trajectory and the final epidemic size.

These results show that unless all individuals are equally likely to be infected, the large-scale effects of heterogeneity on the epidemic trajectory beyond the initial exponential growth cannot be captured by a homogeneous model. In other words, the heterogeneity cannot be coarse-grained into a single effective parameter.

## 2. Heterogeneous connectivity

The SIR model assumes mean-field connectivity (i.e. every individual is equally likely to interact with every other individual). Here we consider a population for which the connectivity within and between groups can be controlled through a clustering parameter between zero and one. A clustering parameter of zero means that the groups are perfectly well-mixed while a clustering parameter of one means that there is no inter-group interactions (mathematical methods can be found in Appendix section 4). Figure 4 shows how connectivity assumptions can affect epidemic size. More important, however, is the space of policy responses that is opened up by the fact that connectivity is not mean-field (i.e. that populations are not well-mixed). The geographic clustering of cases, which can be increased with travel

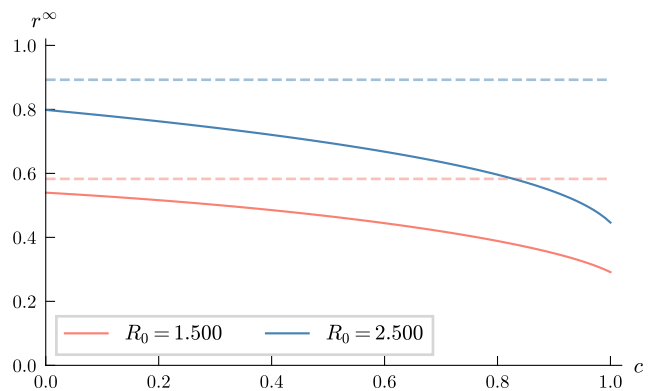


FIG. 4. Effect of heterogeneous connectivity, infectiousness, and susceptibility on the final epidemic size ( $r^\infty$ ). For a given value of  $R_0$ , varying the clustering parameter  $c$  from 0 to 1 (and adjusting the contact parameter  $b_1$  so as to maintain the same value of  $R_0$ ) in a population containing two groups can lead to epidemics of different sizes. The dashed curves of corresponding colors show the epidemic size for the same value of  $R_0$  in the homogeneous SIR model. Parameter values are  $b_2 = 0.9$ ,  $n_1 = n_2 = 0.5$ ,  $\gamma = 1.0$  (see equation 41).

restrictions, can be especially helpful in containing a pandemic using only local, targeted measures [11].

Another large-scale effect of heterogeneity is that the trajectory of the number of infections can have multiple peaks, an impossible occurrence under homogeneous compartmental models (see Figure 5). Of course, the shape of an epidemic trajectory will also be affected by policy interventions, behavioral changes in the population, evolution of the infectious agent, and seasonal effects, as well as nonlinear interactions among and between these factors and various heterogeneities. In Figure 6 (see Appendix), we discuss an observed plateau in the epidemic time-series from India that can be partially explained on the basis of heterogeneity.

## C. Continuous variables and elimination of outbreaks

In compartmental models, which use continuous variables, the number of infections can exponentially decay but will never reach zero. Such models may mischaracterize the effects of temporary, strong interventions by predicting an inevitable “second wave” [26, 27, 36]. Stochastic compartmental models [45] are better suited for analyzing interventions since they use discrete variables and present elimination as a possible scenario (see Appendix section 5 for details).

Stochastic models also show that not all outbreaks grow to become an epidemic [46], an observation which can aid in identifying policies that achieve containment once cases have been brought to a sufficiently low number. The effect of stochasticity can be particularly pronounced if super-spreader events play a substantial role in the overall spread of the disease.

Since stochastic disease transmission events take place through the contact networks of individuals, connectivity patterns can affect the dynamics of elimination. Suspending long-

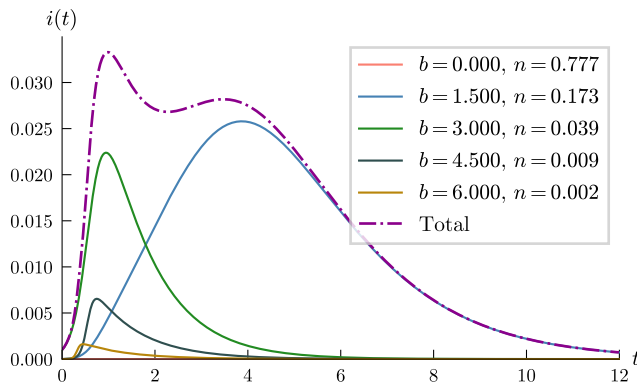


FIG. 5. Heterogeneous connectivity, susceptibility, and infectiousness can substantially change the trajectory of the epidemic. Since the groups are well separated, each group exhibits a unique growth rate. If a homogeneous compartmental model was used to forecast the trajectory at  $t \sim 1.5$ , we would be led to believe that the epidemic was about to end. Parameters:  $c = 0.75$ ,  $\gamma = 1$ , number of groups = 5, contact parameters  $b$  are approximately exponentially distributed with mean 1. Seed infection is in the group with  $b = 3$  (see Appendix section 4b).

range connections (through lock-downs and travel restrictions) can lead to localized epidemics that are largely independent of each other. These local epidemics will be smaller and thus able to be more quickly eliminated. Thus, heterogeneous connectivity can interact with stochastic effects to make elimination a more accessible prospect than homogeneous models would imply.

#### IV. DISCUSSION

What differentiates a good model from a bad model is not its level of detail but rather the relationship between the details included in the model and the most important behaviors of the system. Which details are important can depend not only on the system but also on the modelling objectives. For instance, the precise distribution of generation intervals is crucial if attempting to calculate the reproduction number from the exponential growth/decline rate of an epidemic, but it can generally be coarse-grained to a single time-scale in the context of predicting overall epidemic trajectories.

SEIR models differ from the SIR model in that they use a more detailed and realistic generation interval distribution. The corrections to the epidemic trajectory from the distribution of generation intervals will generally be small compared to other sources of error. Both SIR and SEIR models ignore potentially important factors such as heterogeneity, stochasticity, and behavior change/policy interventions. If such factors are to be ignored, however, the SIR model has the advantage of not including any unnecessary (and therefore potentially misleading) details; its output depends only on the unit-less  $R_0$ , together with a time-scale set by the effective recovery rate  $\gamma$ .

SEIR and related models can provide a breakdown of types of infections and can help with, for example, the management of health care resources (although often, all that matters is the

probability of an infection being of a certain type rather than the precise dynamics between types). However, given the often far larger effects of heterogeneity and stochasticity (not to mention behavioral change and policy response), including the details of disease progression while ignoring these other assumptions may provide a false sense of confidence in the accuracy of the model. More importantly, a misunderstanding of the relative importance of assumptions in any given model may narrow the set of interventions considered.

The idea that some details and assumptions are more important than others is frequently used in mathematics and physics. In mathematics, functions are often approximated locally using a Taylor expansion, with each higher order term providing additional details. A higher order term (finer-grain correction) is used only when all lower-order terms (coarser-grain corrections) have been included. To do otherwise—or to include some corrections at a given scale while ignoring others—is fundamentally unsound and can lead to nonsensical results. When modeling a real-world system, the various details do not necessarily fit cleanly into a Taylor expansion, but the general conceptual principle still holds: details of lower relative importance should be considered only after all of the larger-scale effects have already been taken into account.

Agent-based or network models can transcend some of the limitations of compartmental models. Like any model, however, they may suffer from the flaw of arbitrarily focusing on some details while leaving out others, thereby mischaracterizing the space of large-scale behaviors of the epidemic. As agent-based and network models are generally more detailed, especially careful attention must be paid to this point.

We have not examined many details such as contraction of generation intervals [47], policy responses to an outbreak, temporal and geographic heterogeneity, time varying immunity, seasonal effects, and the emergence of disease variants, among others, which may influence the large-scale behaviors of an epidemic in dramatic ways. The unpredictability inherent to epidemics underscores the need for a precautionary principle for acting under uncertainty [48]. A careful examination of model assumptions is needed, not to evaluate the accuracy of the assumptions themselves—they will always be inaccurate—but to see how they do or do not affect the link between our actions and the space of possible outcomes.

#### Acknowledgements

This material is based upon work supported by the National Science Foundation Graduate Research Fellowship Program under Grant No. 1122374 and by the Hertz Foundation.

#### APPENDIX

##### 1. Epidemic size

The epidemic size is not affected by the generation interval distribution. This can be seen by considering an epidemic process on a graph of  $N$  nodes, where an infected individual has a

chance  $p$  of infecting any other susceptible, and that these infection events are independent of each other. The infected contacts made in this process constitute an Erdos-Renyi graph [15, 16]. Thus, size of the epidemic is the size of the giant component of the Erdos-Renyi graph, the expectation value of which is given by  $z = 1 - \exp(-pNz)$ , which is identical to the epidemic size of the SIR model if  $R_0 = pN$ . Under the assumptions of homogeneity, the epidemic size depends only on  $R_0$ , and not on the generation interval distribution, spreading or recovery rates.

More generally, consider a set of nodes on which each transmission event leads to a directed edge. The transmission events need not be independent (to account for super spreading behavior or heterogeneity). The final size of the epidemic is the number of nodes that are connected directly or indirectly to the seed infection node. So, the final size depends only on the probabilities of transmission (existence of a directed edge between a pair of nodes), and does not depend on the temporal properties of the process such as generation intervals or the number or types of stages in a compartmental model.

## 2. Generation intervals

The SIR model, despite its unrealistic assumptions about the generation interval distribution, can correctly capture the initial exponential growth rate, the basic reproduction number  $R_0$ , and the epidemic size (subject to the assumption of homogeneity).

A general result is that if the generation intervals of an epidemic are given by a random variable  $T$ , the relationship between the effective reproduction number  $R$  and growth rate is given by

$$R = 1/M_T(-\lambda) \quad (8)$$

where  $M_T(\mu) = \mathbb{E}[e^{\mu T}]$  is the moment generating function of the distribution of  $T$  and  $\lambda$  is the exponent of growth or decline [17]. This relationship is valid for any distribution of generation intervals and applies whenever the population size and number of infections is large enough that stochastic effects can be ignored. (There is also the implicit assumption that  $R$  and the generation interval distribution are roughly constant over the time interval during which exponential growth/decline is observed.)

Within an SIR model, the generation intervals are exponentially distributed with mean  $1/\gamma$ , so equation (8) yields

$$R_0 = 1 + \lambda_0/\gamma \quad (9)$$

where  $\lambda_0$  is the initial exponential growth rate. If an SIR model is to accurately describe  $R_0$  and  $\lambda_0$  for an observed epidemic, then  $\gamma$  is determined by Equation (9). But since actual generation intervals are not exponentially distributed, the inverse recovery rate  $1/\gamma$  can not be estimated as the mean of the observed generation intervals. Instead,  $\gamma$  (and  $\beta$ ) serve as effective parameters that coarse-grain the actual distribution of generation intervals  $T$  in such a way that the SIR model yields the correct initial growth rate  $\lambda_0$  and basic reproduction number  $R_0$ :

$$\gamma = \frac{\lambda_0}{R_0 - 1} = \frac{\lambda_0}{1/M_T(-\lambda_0) - 1} \neq \frac{1}{\mathbb{E}[T]} \quad (10)$$

$$\beta = \gamma R_0 = \frac{\lambda_0}{1 - M_T(-\lambda_0)} \quad (11)$$

Nonetheless, much of the modeling literature (e.g. [18–36]) uses  $\gamma = \frac{1}{\mathbb{E}[T]}$ .

## 3. The SEIR model

The SEIR model is an enhanced SIR model where a new compartment of exposed individuals (who have been infected but are not infectious) is introduced. Exposed individuals transition to the infectious compartment at a rate  $\sigma$ . The model is described these differential equations:

$$\frac{ds}{dt} = -\beta si \quad (12)$$

$$\frac{de}{dt} = \beta si - \sigma e \quad (13)$$

$$\frac{di}{dt} = \sigma e - \alpha i \quad (14)$$

$$\frac{dr}{dt} = \alpha i \quad (15)$$

Convolving the two exponential distributions corresponding to the transitions from exposed to infectious and infectious to recovered [17] gives the following distribution of generation intervals

$$g(t) = \frac{\sigma\alpha}{\sigma - \alpha}(e^{-\alpha t} + e^{-\sigma t}) \quad (16)$$

which, when combined with equation (8), yields

$$R_0 = (1 + \lambda_0/\sigma)(1 + \lambda_0/\alpha) \quad (17)$$

where  $\lambda_0$  is the initial exponential growth rate and  $R_0$  is the basic reproduction number. Combining equations (17) and (9) allows us to find an effective  $\gamma$  of the SIR model in terms of the effective parameters of the SEIR model such that the basic reproduction number and the initial growth rate of both the models are equal:

$$R_0 = (1 + \lambda_0/\sigma)(1 + \lambda_0/\alpha) = 1 + \lambda_0/\gamma \quad (18)$$

Thus, any SEIR model can be replaced with an SIR model with the same initial growth rate and  $R_0$  (and thus final size). (Note that for both models,  $\beta$  is also an effective parameter: for the SEIR model,  $\beta = R_0\alpha$ , while for the SIR model,  $\beta = R_0\gamma$ ) The two models will differ only in terms of the precise timing the epidemic curve later on in its trajectory, but such differences will be swamped by other sources of error such as heterogeneity and stochasticity.



#### 4. Heterogeneity

Heterogeneity in infectiousness, susceptibility and connectivity that were explored in section III B use a common framework in which a population of size  $N$  is divided into multiple groups. For a group  $k$ : size of the group is  $N_k$  and the density is  $n_k = N_k/N$ . The number of susceptible, infected and recovered individuals is  $S_k, I_k, R_k$  respectively and their corresponding densities are  $s_k = S_k/N, i_k = I_k/N, r_k = R_k/N$ , such that  $s_k + i_k + r_k = n_k$ . For two groups  $k$  and  $l$ , the inter group interactions (infectiousness, susceptibility and connectivity) are captured by  $B_{kl}$ . The modified SIR equations can be written as:

$$\frac{di_k}{dt} = s_k \sum_l B_{kl} i_l - \gamma i_k \quad (19)$$

$$\frac{ds_k}{dt} = -s_k \sum_l B_{kl} i_l \quad (20)$$

$$\frac{dr_k}{dt} = \gamma i_k \quad (21)$$

It can be seen that a system state with no infections ( $i_k^* = 0$  for all  $k$ ) is a fixed point of these equations. At the beginning of the epidemic, the number of infections in each group will be approximately zero ( $i_k \approx 0$ ) and most of the population will be susceptible ( $s_k \approx n_k$ ). Thus equation (19) can be linearized about the fixed point  $i_k^* = 0$  to give

$$\frac{di_k}{dt} = n_k \sum_l B_{kl} i_l - \gamma i_k \quad (22)$$

This is a set of linear differential equations whose initial time behaviour can be understood from the eigenvalues of the matrix  $M$  where  $M_{kl} = n_k B_{kl} - \gamma \delta_{kl}$ . More precisely, the top eigenvalue of  $M$  gives the initial exponential growth rate of number of infections. As the epidemic progresses, the fraction of infected population is no longer close to zero and the epidemic deviates from exponential growth.

The basic reproduction number is the top eigenvalue of the next generation matrix [49, 50]. The next generation matrix  $G$  is given by

$$G_{kl} = \frac{n_k B_{kl}}{\gamma} \quad (23)$$

The next generation matrix can also be obtained from the matrix  $M$  using  $G = 1 + \frac{1}{\gamma} M$ . Thus the basic reproduction number can be computed using equation (9).

The size of the epidemic  $r_k(t \rightarrow \infty)$  can be estimated by using equations (20) and (21), integrating from  $t = 0$  to  $\infty$ , with the condition that  $i_k(t \rightarrow \infty) = 0$ .

$$r_k^\infty = n_k \left[ 1 - \exp \left\{ -\frac{1}{\gamma} \sum_l B_{kl} r_l^\infty \right\} \right] \quad (24)$$

$$r^\infty = \sum_k r_k^\infty \quad (25)$$

##### a. Heterogeneity in individual characteristics

The following equations were used for the three cases described in section III B 1 of the main text and give expressions for the initial exponential growth rate  $\lambda_0$ , the basic reproduction number  $R_0$  and final epidemic size.

Case I: Heterogeneous infectiousness and homogeneous susceptibility ( $B_{kl} = \beta_k$ ).

$$\lambda_0 = \sum_k n_k \beta_k - \gamma \quad (26)$$

$$= \langle \beta \rangle - \gamma \quad (27)$$

$$R_0 = 1 + \lambda_0 / \gamma = \langle \beta \rangle / \gamma \quad (28)$$

$$\frac{r_k^\infty}{n_k} = 1 - \exp \left\{ -\frac{\langle \beta \rangle r_k^\infty}{\gamma n_k} \right\} \quad (29)$$

$$\frac{r_k^\infty}{n_k} = r_{\text{SIR}}^\infty \quad (30)$$

By selecting the effective spreading rate  $\beta_{\text{SIR}} = \langle \beta \rangle$ , the initial growth rate and basic reproduction number can be reproduced by an SIR model.

Case II: Heterogeneous susceptibility and homogeneous infectiousness ( $B_{kl} = \bar{\beta} \eta_k$ )

$$\lambda_0 = \bar{\beta} \sum_k n_k \eta_k - \gamma \quad (31)$$

$$= \bar{\beta} \langle \eta \rangle - \gamma \quad (32)$$

$$R_0 = 1 + \lambda_0 / \gamma = \bar{\beta} \langle \eta \rangle / \gamma \quad (33)$$

$$\frac{r_k^\infty}{n_k} = 1 - \exp \left\{ -\frac{\bar{\beta} \eta_k}{\gamma} \sum_l r_l^\infty \right\} \quad (34)$$

By selecting the effective spreading rate  $\beta_{\text{SIR}} = \bar{\beta} \langle \eta \rangle$ , the initial growth rate and basic reproduction number can be reproduced by an SIR model.

Case III: Heterogeneous susceptibility and infectiousness ( $B_{kl} = b_k b_l$ )

$$\lambda_0 = \sum_k n_k b_k^2 - \gamma \quad (35)$$

$$= \langle b^2 \rangle - \gamma \quad (36)$$

$$R_0 = 1 + \lambda_0 / \gamma = \langle b^2 \rangle / \gamma \quad (37)$$

$$\frac{r_k^\infty}{n_k} = 1 - \exp \left\{ -\frac{b_k}{\gamma} \sum_l b_l r_l^\infty \right\} \quad (38)$$

By selecting the effective spreading rate  $\beta_{\text{SIR}} = \bar{\beta} \langle \eta \rangle$ , the initial growth rate and basic reproduction number can be reproduced by an SIR model. In all three cases, the final size equations can be solved numerically to compute  $r^\infty$ .

*b. Heterogeneous connectivity*

In the previous section above, the rate  $B_{kl}$  at which an individual in group  $k$  infects an individual in group  $l$  can be described solely in terms of the individual characteristics of members of groups  $k$  and  $l$ . But in reality, connectivity patterns tend to be clustered. In order to capture some of these clustering effects (albeit in a simplified manner), we allow for a higher probability of the disease spreading within groups than between groups. For instance, it is generally more likely for the disease to spread between two individuals living within the same city than between individuals living in different cities.

To account for this, we let  $B_{kl} = b_k b_l C_{kl}$  with  $C_{kl}$  given by

$$C_{kl} = 1 - c + \frac{c}{n_k} \delta_{kl} \quad (39)$$

where  $c \in [0, 1]$  is the clustering parameter. Note that  $C_{kl}$  is normalized such that

$$\sum_l n_l C_{kl} = 1 \quad (40)$$

In Figure 4 of the main text, we explore the case of two groups with different contact parameters  $b_1$  and  $b_2$  and a connectivity parameter  $c$ . The basic reproduction number  $R_0$  is then given by

$$R_0 = \frac{1}{2\gamma} (n_1 B_1 + n_2 B_2 + \sqrt{(n_1 B_1 - n_2 B_2)^2 + 4n_1 n_2 B_c^2}) \quad (41)$$

where  $B_1 = b_1^2(1 - c + c/n_1)$ ,  $B_2 = b_2^2(1 - c + c/n_2)$ , and  $B_c = b_1 b_2(1 - c)$ .

Heterogeneity in the population can cause epidemic trajectories to deviate from simple trajectories (growth and decline), as shown in Figure 5 of the main text. One such deviation is a plateau in the epidemic trajectory observed in both simulations [51] and epidemic data. Figure 6 shows such a plateau in the second wave of COVID-19 epidemic in Chhattisgarh, India.

## 5. Stochasticity

Elimination of an epidemic is a large-scale behavior with very an important implication: unless new cases are imported, a new wave of infections can not occur, thereby paving the way for a safe relaxation of interventions. Continuous models do not exhibit elimination behavior. Stochastic models show that if the effective reproductive number is held below 1, elimination will eventually occur (see Figure 7).

For Figure 7, we use the discrete time Markov chain (DTMC) formulation for simulating the stochastic epidemic [45]. A discrete population of size  $N$  is described by the state  $(S, I)$ , where  $S$  is the number of susceptible and  $I$  is the number of infected individuals. Similar to the deterministic SIR model,  $\beta$  and  $\gamma$  are the effective spreading and recovery rates. The simulation starts with a single infected individual (the population is in a state  $(N - 1, 1)$ ), and at each successive time step the system can tran-

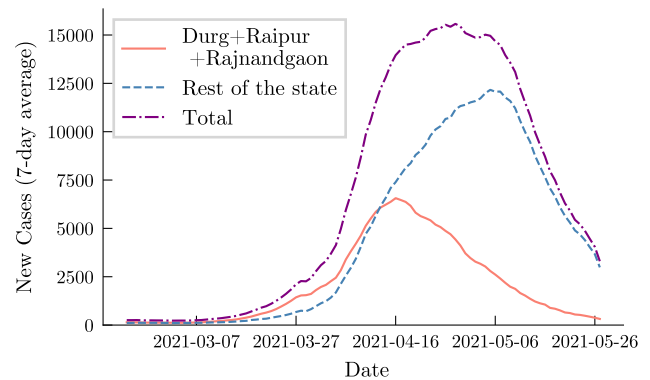


FIG. 6. Time series of new COVID-19 infections from the state of Chhattisgarh in India shows an epidemic plateau between 2021-04-16 and 2021-05-06. Three districts of the state (out of 27), Durg, Raipur and Rajnandgaon peaked around 2021-04-16, while the rest of the districts in the state peaked around 2021-05-06. Such a disparity in the trajectories is a result of the heterogeneity in the social contact structures as well as timing and severity of the interventions. The homogeneous compartmental models when used at the scale of the state will not be able to capture the space of possible trajectories that arise out of heterogeneity. Epidemic data was obtained from [52].

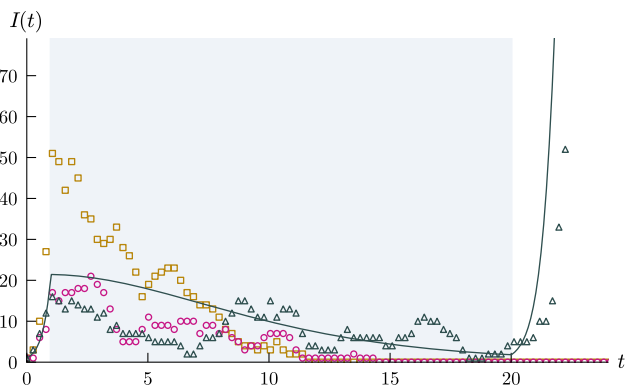


FIG. 7. Continuous compartmental models forecast a deterministic second wave of infections. The shaded region of the plot shows the time period for which intervention is imposed by reducing the spreading rate. The blue curve shows the trajectory of number of infections in the SIR model: After interventions are removed, the infections rise again. The scatter plot trajectory shows the number of cases in the stochastic SIR model, with each marker type corresponding to a single realization of the model. The trajectories with the pink and yellow squares show that there is a finite probability for the epidemic to be eliminated after the intervention and that a second wave does not always occur. Due to the stochastic nature of disease spread, interventions cannot be held in place for a pre-determined amount of time but rather must be calibrated to real-time observations. For instance, for the case of the pink circles and yellow squares, the interventions could be lifted earlier than they were in this simulation, while for the blue triangles, the interventions would need to be kept in place for longer. Simulation parameters:  $\beta = 4.1$ ,  $\gamma = 1$ ,  $N = 1000$ . The spreading rate  $\beta$  is reduced by a factor of 4 during lockdown period which lasts from  $t = 1.0$  to  $t = 20.0$ . The time step used is  $\Delta t = 0.00017$ .



sition to either one of the two states: (a) a susceptible individual becomes infected, (b) an infected individual recovers; or the system can remain in the same state. The transition probabilities for each of these scenarios, when the system is in a state  $(S, I)$ , are:

$$P(S - 1, I + 1) = \beta \frac{SI}{N} \Delta t \quad (42)$$

$$P(S, I - 1) = \gamma I \Delta t \quad (43)$$

$$P(S, I) = 1 - \left( \beta \frac{S}{N} + \gamma \right) I \Delta t \quad (44)$$

where  $\Delta t$  is the time step for the simulation. Its value must be selected such that all transition probabilities lie between zero and one.

- 
- [1] Hethcote, H. W. The mathematics of infectious diseases. *SIAM review* **42**, 599–653 (2000).
- [2] Rock, K., Brand, S., Moir, J. & Keeling, M. J. Dynamics of infectious diseases. *Reports on Progress in Physics* **77**, 026602 (2014). URL <https://doi.org/10.1088/0034-4885/77/2/026602>.
- [3] Barrat, A., Barthelemy, M. & Vespignani, A. *Dynamical Processes on Complex Networks* (Cambridge University Press, 2008). URL <https://doi.org/10.1017/cbo9780511791383>.
- [4] Pastor-Satorras, R., Castellano, C., Mieghem, P. V. & Vespignani, A. Epidemic processes in complex networks. *Reviews of Modern Physics* **87**, 925–979 (2015). URL <https://doi.org/10.1103/revmodphys.87.925>.
- [5] Billah, M. A., Miah, M. M. & Khan, M. N. Reproductive number of coronavirus: A systematic review and meta-analysis based on global level evidence. *PLOS ONE* **15**, e0242128 (2020). URL <https://journals.plos.org/plosone/article?id=10.1371/journal.pone.0242128>.
- [6] Tolles, J. & Luong, T. Modeling epidemics with compartmental models. *JAMA* **323**, 2515 (2020). URL <https://doi.org/10.1001/jama.2020.8420>.
- [7] Weisstein, E. W. Kermack-Mckendrick model. <https://mathworld.wolfram.com/Kermack-McKendrickModel.html>. Accessed: 2021-04-17.
- [8] Roberts, M., Andreasen, V., Lloyd, A. & Pellis, L. Nine challenges for deterministic epidemic models. *Epidemics* **10**, 49–53 (2015). URL <https://doi.org/10.1016/j.epidem.2014.09.006>.
- [9] Siegenfeld, A. F. & Bar-Yam, Y. An introduction to complex systems science and its applications. *Complexity* **2020**, 1–16 (2020). URL <https://doi.org/10.1155/2020/6105872>.
- [10] Siegenfeld, A. F., Taleb, N. N. & Bar-Yam, Y. Opinion: What models can and cannot tell us about COVID-19. *Proceedings of the National Academy of Sciences* **117**, 16092–16095 (2020). URL <https://doi.org/10.1073/pnas.2011542117>.
- [11] Siegenfeld, A. F. & Bar-Yam, Y. The impact of travel and timing in eliminating COVID-19. *Communications Physics* **3** (2020). URL <https://doi.org/10.1038/s42005-020-00470-7>.
- [12] Miller, J. C. A note on the derivation of epidemic final sizes. *Bulletin of Mathematical Biology* **74**, 2125–2141 (2012). URL <https://doi.org/10.1007/s11538-012-9749-6>.
- [13] Andreasen, V. The final size of an epidemic and its relation to the basic reproduction number. *Bulletin of Mathematical Biology* **73**, 2305–2321 (2011). URL <https://doi.org/10.1007/s11538-010-9623-3>.
- [14] Ma, J. & Earn, D. J. D. Generality of the final size formula for an epidemic of a newly invading infectious disease. *Bulletin of Mathematical Biology* **68**, 679–702 (2006). URL <https://doi.org/10.1007/s11538-005-9047-7>.
- [15] Ball, F., Mollison, D. & Scalia-Tomba, G. Epidemics with two levels of mixing. *The Annals of Applied Probability* 46–89 (1997).
- [16] Barbour, A. & Mollison, D. Epidemics and random graphs. In *Stochastic processes in epidemic theory*, 86–89 (Springer, 1990).
- [17] Wallinga, J. & Lipsitch, M. How generation intervals shape the relationship between growth rates and reproductive numbers. *Proceedings of the Royal Society B: Biological Sciences* **274**, 599–604 (2006). URL <https://doi.org/10.1098/rspb.2006.3754>.
- [18] Choi, S. & Ki, M. Estimating the reproductive number and the outbreak size of COVID-19 in Korea. *Epidemiology and Health* **42**, e2020011 (2020). URL <https://doi.org/10.4178/epih.e2020011>.
- [19] Hyafil, A. & Morina, D. Analysis of the impact of lockdown on the reproduction number of the SARS-Cov-2 in Spain. *Gaceta Sanitaria* (2020). URL <https://doi.org/10.1016/j.gaceta.2020.05.003>.
- [20] Kuniya, T. Prediction of the epidemic peak of coronavirus disease in Japan, 2020. *Journal of Clinical Medicine* **9**, 789 (2020). URL <https://doi.org/10.3390/jcm9030789>.
- [21] Read, J. M., Bridgen, J. R., Cummings, D. A., Ho, A. & Jewell, C. P. Novel coronavirus 2019-nCoV: early estimation of epidemiological parameters and epidemic predictions (2020). URL <https://doi.org/10.1101/2020.01.23.20018549>.
- [22] Tang, B. *et al.* Estimation of the transmission risk of the 2019-nCoV and its implication for public health interventions. *Journal of Clinical Medicine* **9**, 462 (2020). URL <https://doi.org/10.3390/jcm9020462>.
- [23] Wu, J. T., Leung, K. & Leung, G. M. Nowcasting and forecasting the potential domestic and international spread of the 2019-nCoV outbreak originating in Wuhan, China: a modelling study. *The Lancet* **395**, 689–697 (2020). URL [https://doi.org/10.1016/s0140-6736\(20\)30260-9](https://doi.org/10.1016/s0140-6736(20)30260-9).
- [24] Zhou, H. *et al.* Characterizing the transmission and identifying the control strategy for COVID-19 through epidemiological modeling (2020). URL <https://doi.org/10.1101/2020.02.24.20026773>.
- [25] Kyrychko, Y. N., Blyuss, K. B. & Brovchenko, I. Mathematical modelling of the dynamics and containment of COVID-19 in Ukraine. *Scientific Reports* **10** (2020). URL <https://doi.org/10.1038/s41598-020-76710-1>.
- [26] Walker, P. G. T. *et al.* The impact of COVID-19 and strategies for mitigation and suppression in low- and middle-income countries. *Science* eabc0035 (2020). URL <https://doi.org/10.1126/science.abc0035>.
- [27] Davies, N. G. *et al.* Effects of non-pharmaceutical interventions on COVID-19 cases, deaths, and demand for hospital services in the UK: a modelling study. *The Lancet Public Health* **5**, e375–e385 (2020). URL [https://doi.org/10.1016/s2468-2667\(20\)30133-x](https://doi.org/10.1016/s2468-2667(20)30133-x).

- [28] Chowdhury, R. *et al.* Dynamic interventions to control COVID-19 pandemic: a multivariate prediction modelling study comparing 16 worldwide countries. *European Journal of Epidemiology* **35**, 389–399 (2020). URL <https://doi.org/10.1007/s10654-020-00649-w>.
- [29] Rădulescu, A., Williams, C. & Cavanagh, K. Management strategies in a SEIR-type model of COVID 19 community spread. *Scientific Reports* **10** (2020). URL <https://doi.org/10.1038/s41598-020-77628-4>.
- [30] Scala, A. *et al.* Time, space and social interactions: exit mechanisms for the Covid-19 epidemics. *Scientific Reports* **10** (2020). URL <https://doi.org/10.1038/s41598-020-70631-9>.
- [31] Balabdaoui, F. & Mohr, D. Age-stratified discrete compartment model of the COVID-19 epidemic with application to Switzerland. *Scientific Reports* **10** (2020). URL <https://doi.org/10.1038/s41598-020-77420-4>.
- [32] Balcan, D. *et al.* Multiscale mobility networks and the spatial spreading of infectious diseases. *Proceedings of the National Academy of Sciences* **106**, 21484–21489 (2009). URL <https://doi.org/10.1073/pnas.0906910106>.
- [33] Balcan, D. *et al.* Modeling the spatial spread of infectious diseases: The GLocal epidemic and mobility computational model. *Journal of Computational Science* **1**, 132–145 (2010). URL <https://doi.org/10.1016/j.jocs.2010.07.002>.
- [34] Chinazzi, M. *et al.* The effect of travel restrictions on the spread of the 2019 novel coronavirus (COVID-19) outbreak. *Science* **368**, 395–400 (2020). URL <https://doi.org/10.1126/science.aba9757>.
- [35] Domenico, L. D., Pullano, G., Sabbatini, C. E., Boëlle, P.-Y. & Colizza, V. Impact of lockdown on COVID-19 epidemic in Île-de-France and possible exit strategies. *BMC Medicine* **18** (2020). URL <https://doi.org/10.1186/s12916-020-01698-4>.
- [36] Ferguson, N. *et al.* Report 9: Impact of non-pharmaceutical interventions (NPIs) to reduce COVID19 mortality and healthcare demand (2020). URL <http://spiral.imperial.ac.uk/handle/10044/1/77482>.
- [37] Girvan, M. & Newman, M. E. J. Community structure in social and biological networks. *Proceedings of the National Academy of Sciences* **99**, 7821–7826 (2002). URL <https://doi.org/10.1073/pnas.122653799>.
- [38] Arenas, A., Danon, L., Diaz-Guilera, A., Gleiser, P. M. & Guimera, R. Community analysis in social networks. *The European Physical Journal B* **38**, 373–380 (2004).
- [39] Hedayatifar, L., Rigg, R. A., Bar-Yam, Y. & Morales, A. J. US social fragmentation at multiple scales. *Journal of The Royal Society Interface* **16**, 20190509 (2019). URL <https://doi.org/10.1098/rsif.2019.0509>.
- [40] Britton, T., Ball, F. & Trapman, P. A mathematical model reveals the influence of population heterogeneity on herd immunity to SARS-CoV-2. *Science* **369**, 846–849 (2020). URL <https://doi.org/10.1126/science.abc6810>.
- [41] Gou, W. & Jin, Z. How heterogeneous susceptibility and recovery rates affect the spread of epidemics on networks. *Infectious Disease Modelling* **2**, 353–367 (2017). URL <https://doi.org/10.1016/j.idm.2017.07.001>.
- [42] Gerasimov, A., Lebedev, G., Lebedev, M. & Semenycheva, I. COVID-19 dynamics: A heterogeneous model. *Frontiers in Public Health* **8** (2021). URL <https://doi.org/10.3389/fpubh.2020.558368>.
- [43] Hickson, R. & Roberts, M. How population heterogeneity in susceptibility and infectivity influences epidemic dynamics. *Journal of Theoretical Biology* **350**, 70–80 (2014). URL <https://doi.org/10.1016/j.jtbi.2014.01.014>.
- [44] Dolbeault, J. & Turinici, G. Social heterogeneity and the COVID-19 lockdown in a multi-group SEIR model. *Computational and Mathematical Biophysics* **9**, 14–21 (2021). URL <https://doi.org/10.1515/cmb-2020-0115>.
- [45] Allen, L. J. S. An introduction to stochastic epidemic models. In *Mathematical Epidemiology*, 81–130 (Springer Berlin Heidelberg, 2008). URL [https://doi.org/10.1007/978-3-540-78911-6\\_3](https://doi.org/10.1007/978-3-540-78911-6_3).
- [46] Althouse, B. M. *et al.* Superspreading events in the transmission dynamics of SARS-CoV-2: Opportunities for interventions and control. *PLOS Biology* **18**, e3000897 (2020). URL <https://doi.org/10.1371/journal.pbio.3000897>.
- [47] Kenah, E., Lipsitch, M. & Robins, J. M. Generation interval contraction and epidemic data analysis. *Mathematical Biosciences* **213**, 71–79 (2008). URL <https://doi.org/10.1016/j.mbs.2008.02.007>.
- [48] Cirillo, P. & Taleb, N. N. Tail risk of contagious diseases. *Nature Physics* **16**, 606–613 (2020). URL <https://doi.org/10.1038/s41567-020-0921-x>.
- [49] Diekmann, O., Heesterbeek, J. & Metz, J. On the definition and the computation of the basic reproduction ratio  $R_0$  in models for infectious diseases in heterogeneous populations. *Journal of Mathematical Biology* **28** (1990). URL <https://doi.org/10.1007/bf00178324>.
- [50] Van den Driessche, P. & Watmough, J. Reproduction numbers and sub-threshold endemic equilibria for compartmental models of disease transmission. *Mathematical biosciences* **180**, 29–48 (2002).
- [51] Maltsev, A. V. & Stern, M. D. Social heterogeneity drives complex patterns of the COVID-19 pandemic: Insights from a novel stochastic heterogeneous epidemic model (SHEM). *Frontiers in Physics* **8** (2021). URL <https://doi.org/10.3389/fphy.2020.609224>.
- [52] Covid19india. <https://www.covid19india.org/>. Accessed: 2021-05-27.